Consolidated Al/Al_2O_3 Nanocomposites by Equal Channel Angular Pressing and Hot Extrusion

Riccardo Casati[1], Maurizio Vedani[1], David Dellasega[2], Paola Bassani[3], and Ausonio Tuissi[3]

[1]*Department of Mechanical Engineering, Politecnico di Milano, Milano, Italy*
[2]*Department of Energy, Politecnico di Milano, Milano, Italy*
[3]*CNR-IENI, Lecco, Italy*

Introduction

Aluminum composites reinforced with ceramic particles are very attractive materials for industrial applications requiring light weight, high specific strength and elastic modulus, good tribological and damping properties [1]. The mechanical behavior of these metal matrix composites can be further improved by using nanoceramic particles as a replacement for conventional microsized reinforcements [2–4]. Such small particulates in metal matrix nanocomposites (MMNCs) are more efficient in enhancing mechanical performance as they act to pin dislocations, hindering the movement of these lattice defects [5, 6]. In recent investigations [2–4], material strengthening through the dispersion of different kinds of oxides, carbides, and other ceramic materials was achieved by different preparation methods. Moreover, carbon nanotubes which are characterized by very high strength, stiffness, and electrical conductivity are good reinforcements since they can additionally confer to the base metal interesting physical properties suitable for advanced applications, such as for electrical devices [4, 7–11]. The poor wettability of ceramic particulates is the main problem in MMNC production. In order to overcome this obstacle, several non-conventional fabrication processes were proposed in recent studies. Ultrasound assisted casting [12], disintegrated melt deposition [2], in situ processing [13, 14], powder metallurgy (PM) [15–19], and other methods [20, 21] have proven to be effective in preparing MMNCs characterized by well-dispersed discrete nanoparticles. Common consolidation techniques used for these materials include hot forging and hot isostatic pressing (HIP) [2]. The present work focuses on the preparation process by PM route of aluminum based MMNCs reinforced with different amounts of γ-Al2O3. Powders were mixed and ground by high-energy ball milling and then compacted through equal channel angular pressing (ECAP) and by hot extrusion (HE). This work differs from Haghighi's work [16] because HE has been used for powder compaction at low temperature (300°C), while in Ref. [16] powders were sintered in a furnace at high temperature (540°C) and then hot extruded. The use of a significantly lower processing temperature allows retaining a finer grain structure of the matrix, as it is inherited from the milling process. A combination of ECAP and HE was also evaluated as possible process for production of composite. Moreover, in this work, particles dispersion is considerably simpler since it was carried out by dry high-energy ball milling, while in Ref. [16] powders were mixed in ethanol, sonicated, and wet attritioned. Investigations of the microstructure were carried out by scanning electron microscope (SEM) and X-ray diffraction (XRD) at different stages of the process. The physical properties in terms of density and Vickers hardness of the sample produced by ECAP and HE were compared in order to select the most suitable PM process for the production of MMNCs.

Received February 14, 2014; Accepted March 4, 2014

Address correspondence to Riccardo Casati, Department of Mechanical Engineering, Politecnico di Milano, Via La Masa, 20156, Milano, Italy; E-mail: riccardo.casati@polimi.it

Color versions of one or more of the figures in the article can be found online.

Materials and methods

Pure aluminum powder (supplied by ECKA Granules GmbH, Germany) and cubic alumina γ-Al_2O_3 (supplied by COMETOX Srl, Italy), with average size of 20 μm and 20 nm, respectively, were employed for this investigation. High-energy ball milling was carried out in order

to mix 2% and 5% (weight fraction) of alumina in aluminum powder and to break up Al_2O_3 clusters. This was conducted using a Vario-Planetary Mill Pulverisette 4 equipped by tempered steel bowls and balls (10 mm in diameter). The ball-to-powder weight ratio was 5:1 and 1% vol. of ethanol was added as process control agent (PCA) to avoid excessive cold welding and agglomeration of powders. The bowls were packed and enclosed within an argon atmosphere to prevent the oxidation of powder. The ball milling was performed for 5 h, with interruptions every 30 min for 15 min to avoid excessive heating of the powder. The speed of the main disk was set to 250 rpm clockwise whereas the speed of the two planets was set to 200 rpm counter-clockwise. Powder compaction was performed on as-received and ball milled pure aluminum, as well as the Al/Al_2O_3 blended powder. These powders were first pressed manually into cylindrical containers (external diameter = 10 mm, internal diameter = 8 mm), before being closed by a plug and subjected to either ECAP, HE, or a combined ECAP +HE process. The ECAP die used for the experiments had a channel intersection angle of 110° and a channel diameter of 10 mm. The ECAP process was performed at 200°C following route Bc (rotation of the billet by 90° clockwise after each pass) for three passes. The HE process was conducted at 300°C with the starting billet reducing from an initial diameter of 10 mm to a final diameter of 4 mm. The extrusion die was heated by an induction coil and the temperature was controlled by a set of thermocouples [22]. It was not possible to perform HE at lower temperatures since the required load exceeded the maximum load for the employed press (100 kN). Both the processes were carried out at constant speed of 5 mm/min. A secondary process of HE was performed on ECAP samples using the same working parameters stated above. The density of the materials was estimated based on the Archimedes' principle using polished samples. The Vickers microhardness (HV) was measured by means of a Future Tech Corp. FM-700 tester applying 1 N load for 15 s, with 10 measurements taken for each sample. PANalytical X'pert Pro was employed for XRD investigations. Microstructural analysis was carried out by SEM Zeiss Supra 40 equipped with Gemini column, In-lens detector, Everhart-Thornley secondary electron detector, back-scattered electron detector, and microanalysis apparatus for energy-dispersive X-ray spectroscopy (EDS) elemental analysis.

Results and discussion

A preliminary SEM investigation on as-received powders revealed that the alumina nanoparticles were aggregated in spherical microsized clusters. In contrast, aluminum powders were well detached and roughly of spherical shape (Fig. 1). High-energy ball milling processing was carried out on Al/Al_2O_3 blend of powders to break the ceramic aggregates and homogeneously disperse them into the metal particles.

In Fig. 1, the micrographs of pure aluminum particles before ball milling and after 2 and 5 h of the grinding process are presented. The repeated fracture and cold welding due to the continuous collisions between balls and powders leads to the formation of flake-like particulates. The accumulation of lattice defects through this

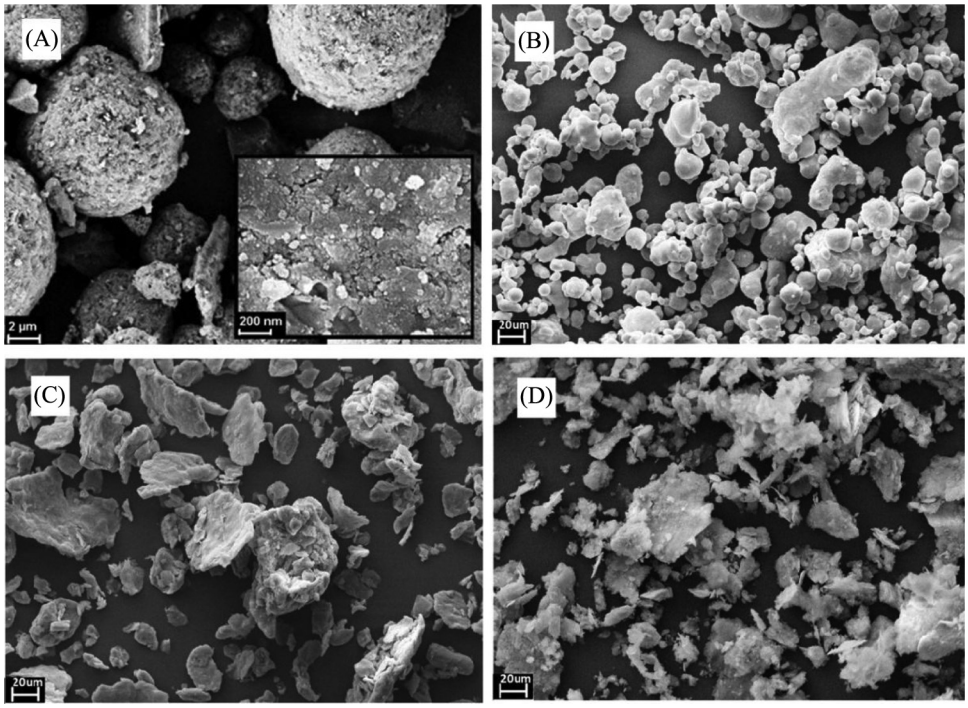

Figure 1.—SEM micrograph (secondary electrons) of (A) Al_2O_3 in the as-received condition (a further magnification of the surface is shown inset); (B) as-received pure aluminum powder; (C) pure aluminum after 2 h of ball milling; and (D) pure aluminum after 5 h of ball milling.

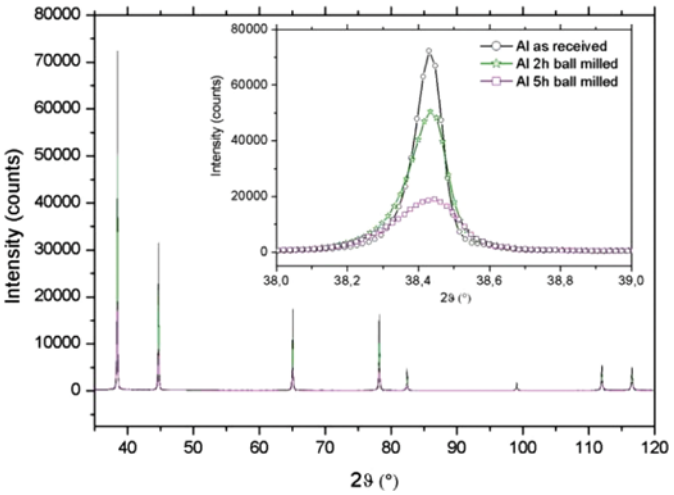

FIGURE 2.—XRD patterns of Al powder in as-received condition and after 2 and 5 h of high-energy ball milling. The magnification of the peak at 38.4° highlights the peak broadening with increasing milling time.

severe plastic deformation (likely in the form of dislocations) is confirmed by XRD analysis. The full diffraction patterns of pure Al powder before and after ball milling are shown in Fig. 2, with a magnified view of the (111) peak at 38.4° inset. The milled powders are characterized by broadened peaks which indicate smaller crystallites and large amount of crystal defects. SEM investigation performed on composite powders (Al with the addition of Al_2O_3) for 2 and 5 h has shown a fairly similar morphological evolution.

Compaction was first carried out on pure aluminum powder in the as-received condition and after 2 h of high-energy ball milling. Table 1 summarizes the results in terms of density and Vickers hardness measured of the consolidated samples. The flaky particles were shown to be more difficult to compact (as inferred from lower density of the compacted). They can withstand a lower amount of deformation and they frequently lead to the formation of bridges between particles and pores. In this respect, the micrograph depicted in Fig. 3 shows the sub-micrometric porosity which characterizes the structure of the sample compacted by ECAP after high-energy ball milling. In the same figure, slight

TABLE 1.—Density and Vickers hardness of pure aluminum (as-received condition and after high-energy ball milling) prepared by ECAP at 200°C and HE at 300°C.

	Density (g/cm^3)	HV (std. dev.)
ECAP pure Al as received	2.69	48.8 (0.3)
ECAP pure Al ball milled	2.67	51.5 (0.7)
HE pure Al as received	2.67	42.6 (0.4)
HE pure Al ball milled	2.66	43.3 (0.3)
ECAP + HE pure Al as received	2.68	43.0 (0.3)
ECAP + HE pure Al ball milled	2.68	43.6 (0.5)

Theoretical density of aluminum is 2.7 g/cm^3.

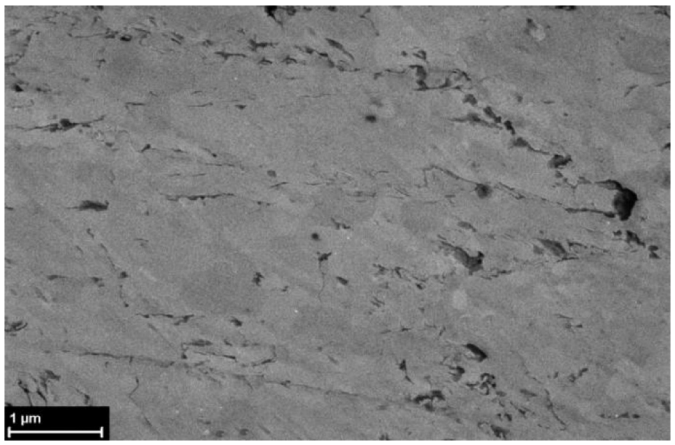

FIGURE 3.—SEM micrograph (secondary electrons) of consolidated milled aluminum powders.

differences in conductivity makes it possible to detect the distinct crystal grains. Their average size is on the order of less than 1 μm. In spite of the lower density, the samples subjected to 2 h of milling achieve higher Vickers hardness compared to the samples compacted starting from the as-received powder. This is likely due to the contribution of work hardening and grain refinement conferred by the high-energy milling.

The particles sintered by ECAP exhibit better results in terms of Vickers hardness than the ones compacted by only HE. In addition, they also show improved properties than the specimens that underwent HE after ECAP. This is probably due to the higher processing temperatures of HE (300°C) as compared to that of ECAP (200°C).

Since the best density and hardness results were obtained by compacting pure aluminum powder by ECAP alone, this process was selected to produce aluminum based composites reinforced by 2 and 5 wt% of alumina. The microstructures for these two composites are shown in Figs. 4 and 5, respectively.

For both cases, it appears that the reinforcement nanoparticles are partially aggregated into microclusters (Figs. 4(A) and 5(A)) and partially spread as single nanoparticles (Figs. 4(B) and 5(B)) within the metal matrix. It is accepted that to achieve the best mechanical performance in MMNCs, the particles should be well dispersed throughout the matrix volume. In this way they can be more effective in interacting with dislocations, hampering their motion. Preparatory breakage of alumina clusters by ultra-sonication or longer milling time may lead to a further improvement of the dispersion of ceramic compounds within the metal matrix. Increasing the amount of Al_2O_3 leads to a reduction in composite density (Table 2). Despite the porosity and the alumina clusters, the composites reach higher Vickers hardness compared with the pure aluminum samples (see Tables 1 and 2). In particular, the addition of 2% and 5% of alumina to the base metal entails a hardness of 54.3 and 58.2 HV, respectively. It means

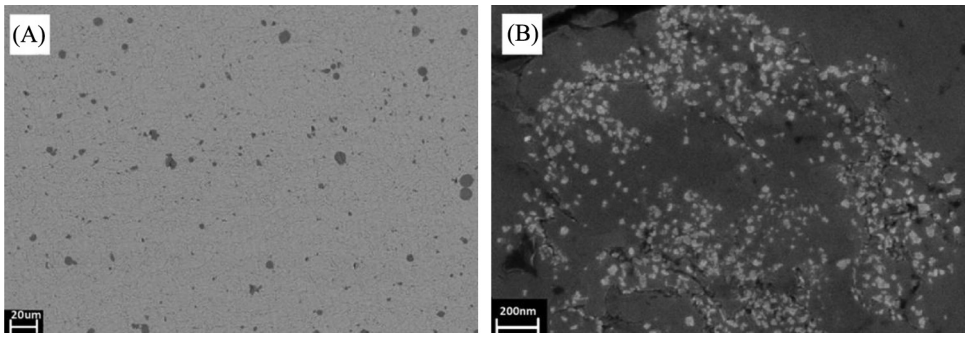

FIGURE 4.—SEM micrographs of Al–2%Al_2O_3 composite (A) at low magnification: presence of microsized alumina clusters (back-scattered detector) and (B) at high magnification: nanoalumina dispersed within the aluminum matrix (secondary electrons).

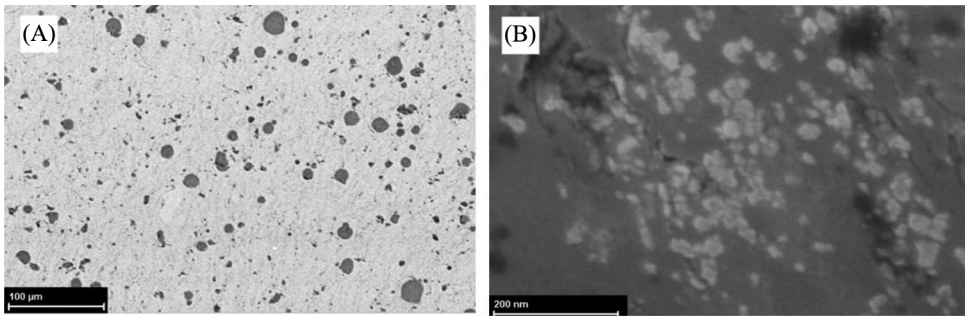

FIGURE 5.—SEM micrographs of Al-5%Al_2O_3 composite (A) low magnification: presence of microsized alumina clusters (back-scattered electrons) and (B) high magnification: nanoalumina dispersed within the aluminum matrix (secondary electrons).

TABLE 2.—Density and Vickers hardness of Al/Al_2O_3 (2 and 5 wt%) composites prepared by ECAP at 200°C.

	Density (g/cm^3)	Vickers hardness (HV)
ECAP Al + 2%Al_2O_3 ball milled	2.63	54.3 (0.6)
ECAP Al + 5%Al_2O_3 ball milled	2.53	58.2 (0.7)

Theoretical density of aluminum is 2.7 g/cm^3. Theoretical density of alumina is 3.9 g/cm^3.

that, the addition of 5% of alumina to the Al matrix leads to a 12% increase in hardness.

CONCLUSIONS

Aluminum based MMNC consisting of Al_2O_3 dispersed within an Al matrix was produced via the PM method and consolidated through ECAP. High-energy ball milling was employed to mix Al/Al_2O_3 powders and to break up the alumina clusters. It led to the formation of flake-like particulates and the introduction of a large amount of crystal defects within the metal powders. Consolidation of pure aluminum powder both before and after ball milling was successfully performed by HE at 300°C and by ECAP at 200°C. A secondary extrusion process was also considered for the ECAP specimens, however the highest Vickers hardness and density was reached when only ECAP was employed (51.5 HV, 2.67 g/cm^3). Aluminum composites reinforced with 2% and 5% of Al_2O_3 nanoparticles prepared by ECAP resulted in regions of micrometer-sized clusters and well as single nanoparticles dispersed throughout the matrix. The increase of the amount of Al_2O_3 involved reduction in composite density. In spite of the increased porosity and Al_2O_3 clusters, the composites reached higher Vickers hardness compared to pure aluminum samples. The addition of 5% of alumina to the Al matrix led to an increase in hardness of 12%. Preliminary breakage of clusters by ultrasonication or by longer milling times may help in achieving an improved dispersion of the ceramic reinforcement phase within the metal matrix so as to fully exploit the reinforcement strengthening and to obtain improved mechanical performance of the final composite.

REFERENCES

1. Kainer, K.U. *Metal Matrix Composites. Custom-made Materials for Automotive and Aerospace Engineering*; WILEY-VCH Verlag GmbH & Co. KGaA: Weinheim, Germany, 2006.
2. Tjong, S.C. Novel nanoparticle-reinforced metal matrix composites with enhanced mechanical properties. *Advanced Engineering Materials* **2007**, *9* (8), 639–652.
3. Camargo, P.H.C.; Satyanarayana, K.G.; Wypych, F. Nanocomposites: Synthesis, structure, properties and new application opportunities. *Materials Research* **2009**, *12* (1), 1–39.

4. Bakshi, S.R.; Lahiri, D.; Agarwal, A. Carbon nanotube reinforced metal matrix composites – a review. *International Materials Reviews* **2010**, *55* (1), 41–64.
5. Sanaty-Zadeh, A. Comparison between current models for the strength of particulate-reinforced metal matrix nanocomposites with emphasis on consideration of Hall–Petch effect. *Materials Science and Engineering A* **2012**, *531*, 112–118.
6. Zhang, Z.; Chen, D.L.; Contribution of Orowan strengthening effect in particulate-reinforced metal matrix nanocomposites. *Materials Science and Engineering A* **2008**, *483*, 148–152.
7. Yamanaka, S.; Gonda, R.; Kawasaki, A.; Sakamoto, H.; Mekuchi, Y.; Kuno, M.; Tsukada, T. Fabrication and thermal properties of carbon nanotube/nickel composite by spark plasma sintering method. *Materials Transactions* **2007**, *48* (9), 2506–2512.
8. Deng, C.F.; Wang, D.Z.; Zhang, X.X.; Ma, Y.X. Calorimetric study of carbon nanotubes and aluminum. *Materials Letters* **2007**, *61* (14–15), 3221–3223.
9. Deng, C.F.; Wang, D.Z.; Zhang, X.X.; Li, A.B. Processing and properties of carbon nanotubes reinforced aluminum composites. *Materials Science and Engineering A* **2007**, *444*, 138–145.
10. Esawi, A.M.K.; Morsi, K.; Sayed, A.; Abdel Gawad, A.; Borah, P. Fabrication and properties of dispersed carbon nanotube–aluminum composites. *Material Science and Engineering A* **2009**, *508* (1–2), 167–173.
11. Al-Aqeeli, N.; Abdullahi, K.; Suryanarayana, C.; Laoui, T.; Nouari, S. Structure of mechanically milled CNT-reinforced Al-alloy nanocomposites. *Materials and Manufacturing Processes* **2013**, *28* (9), 984–990.
12. Erman, A.; Groza, J.; Li, X.; Choi, H.; Cao, G. Nanoparticle effects in cast Mg-1 wt% SiC nano-composites. *Materials Science and Engineering A* **2012**, *558*, 39–43.
13. Aghilia, S.E.; Enayati, M.H.; Karimzadeha, F. In-situ synthesis of alumina reinforced (Fe,Cr)3Al intermetallic matrix nanocomposite. *Materials and Manufacturing Processes* **2012**, *27* (12), 1348–1353.
14. Adabavazeha, Z.; Karimzadeha, F.; Enayati, M.H. Formation mechanism of nanostructured (Ni, Fe)3Al-Al2O3 nanocomposite and its characterization. *Materials and Manufacturing Processes* **2012**, *27* (6), 626–630.
15. Goussous, S.; Xu, W.; Wu, X.; Xia, K. Al–C nanocomposites consolidated by back pressure equal channel angular pressing. *Composite Science and Technology* **2009**, *69* (11–12), 1997–2001.
16. Haghighi, R.D.; Jahromi, S.A.J.; Moresedgh, A.; Khorshid, M.T. A comparison between ECAP and conventional extrusion for consolidation of aluminum metal matrix composite. *Journal of Materials Engineering and Performance* **2011**, *21* (9), 1885–1892.
17. Goussous, S.; Xu, W.; Xia, K. Developing aluminum nanocomposites via severe plastic deformation. *Journal of Physics, Conference Series* **2010**, *240* (1), 012106.
18. Casati, R.; Amadio, M.; Biffi, C.A.; Dellasega, D.; Tuissi, A.; Vedani, M. Al/Al2O3 nano-composite produced by ECAP. *Material Science Forum* **2013**, *762*, 457–464.
19. Casati, R.; Bonollo, F.; Dellasega, D.; Fabrizi, A.; Timelli, G.; Tuissi, A.; Vedani, M. Ex situ Al–Al2O3 ultrafine grained nanocomposites produced via powder metallurgy. *Journal of Alloys and Compounds* **2013**, http://dx.doi.org/10.1016/j.jallcom.2013.10.236
20. Nie, K.B.; Wang, X.J.; Xu, L.; Wu, K.; Hu, X.S.; Zheng, M.Y. Influence of extrusion temperature and process parameter on microstructures and tensile properties of a particulate reinforced magnesium matrix nanocomposites. *Materials and Design* **2012**, *36*, 199–205.
21. Yan, Z.; Chen, M.; Yang, J.; Yang, L.; Gao, H. Grain refinement of CuNi10Fe1Mn alloy by SiC nanoparticles and electromagnetic stirring. *Materials and Manufacturing Processes* **2013**, *28* (8), 957–961.
22. Ge, Q.; Vedani, M.; Vimercati, G. Extrusion of magnesium tubes for biodegradable stent precursors. *Materials and Manufacturing Processes* **2012**, *27* (2), 140–146.